Published in final edited form as:
J Proteome Res. 2009 March ; 8(3): 1540–1554. doi:10.1021/pr800894p.

Identification of Phosphorylation-Dependent Binding Partners of Aquaporin-2 Using Protein Mass Spectrometry

Nicholas A. Zwang[1], **Jason D. Hoffert**[1], **Trairak Pisitkun**[1], **Hanne B. Moeller**[2], **Robert A. Fenton**[2], and **Mark A. Knepper**[1]

1 *Laboratory of Kidney and Electrolyte Metabolism, National Heart, Lung and Blood Institute, National Institutes of Health, Bethesda, MD 20892, USA*

2*Water and Salt Center, University of Aarhus, Aarhus, Denmark*

Abstract

Vasopressin-mediated control of water permeability in the renal collecting duct occurs in part through regulation of the distribution of aquaporin-2 (AQP2) between the apical plasma membrane and intracellular membrane compartments. Phosphorylation of Ser-256 at AQP2's cytoplasmic COOH-terminus is well-accepted as a critical step for translocation. The aim of this study was to identify binding partners to phosphorylated versus nonphosphorylated forms of the AQP2 COOH-terminus via a targeted comparative proteomic approach. Cytosol from inner medullary collecting ducts isolated from rat kidneys was incubated with "bait" peptides, representing the COOH-terminal AQP2 tail in its nonphosphorylated and phosphorylated forms, to capture differentially-bound proteins prior to LC-MS/MS analysis. Mass spectrometric results were confirmed by immunoblotting. Immunoprecipitation was performed using an AQP2 COOH-terminal antibody combined with immunblotting against the proposed binding partners in order to demonstrate interactions with native AQP2. Our studies confirmed previously identified interactions between AQP2 and hsc70, hsp70−1 and −2, as well as annexin II. These proteins were found to bind less to the Ser-256-phosphorylated AQP2 than to the non-phosphorylated form. In contrast, another heat shock protein, hsp70−5 (BiP/grp78), bound to phosphorylated AQP2 more avidly than to non-phosphorylated AQP2. Immunogold EM studies demonstrated that BiP is present not only in the ER, but in the cytoplasm and apical plasma membrane of rat collecting duct cells. Furthermore, confocal immunofluorescence studies showed partial colocalization of BiP with AQP2 in non-ER compartments. These results suggest that phosphorylation of AQP2 at Ser-256 may regulate AQP2 trafficking in part by mediating differential binding of hsp70 family proteins to the COOH-terminal tail.

Keywords

tandem mass spectrometry; phosphoproteomics; chaperone; affinity chromatography

INTRODUCTION

Vasopressin-regulated trafficking of aquaporin-2 (AQP2) to and from the apical plasma membrane of collecting duct principal cells is a central process in the regulation of renal water excretion [1]. The net amount of AQP2 present in the plasma membrane depends on a dynamic equilibrium between endocytosis and exocytosis of vesicles containing AQP2, both of which are regulated by vasopressin [2-4]. Vasopressin signaling in collecting ducts involves binding

Corresponding author: Mark Knepper, National Institutes of Health, 10 Center Dr, Bldg 10, Room 6N260, Bethesda, MD 20892−1603. Phone: (301) 496−3064; E-mail: E-mail: KnepperM@nhlbi.nih.gov.

of vasopressin to the V2 receptor, which activates adenylyl cyclases, increases intracellular cAMP concentrations, and activates protein kinase A (PKA) [2,5,6]. Acting through cAMP, vasopressin also increases intracellular calcium in collecting duct cells [7] and the vasopressin-mediated increase in osmotic water permeability in the collecting duct is in part dependent on calcium and calmodulin [8,9].

AQP2 is phosphorylated at four sites on its cytoplasmic COOH-terminus: Ser-256, Ser-261, Ser-264, and Ser-269 [10]. Phosphorylation at all four sites has been shown to be regulated by vasopressin [11,12]. Among these sites, phosphorylation at Ser-256 was identified first and has been shown to play a critical role in the trafficking process [13-16]. This is the only one of the four sites that has been shown to be directly phosphorylated by PKA [12].

Hypothetically, regulation of exo- and endocytosis of AQP2-containing vesicles involves interactions with proteins that physically connect AQP2 to motive mechanisms that translocate the vesicles toward and away from the apical plasma membrane. Working with this hypothesis, several groups have identified proteins that bind to AQP2 and play potential roles in trafficking. These proteins include SPA-1 [17], actin [18], hsc70/hsp70 [19], MAL [20], annexin II [21,22], tropomyosin 5b (tropomyosin 1 alpha, isoform h) [23], and AKAP220 [24]. One way that vasopressin could control trafficking is to affect the binding of these or other proteins to the COOH-tail of AQP2 through changes in binding affinities resulting from regulated phosphorylation. Thus, an important objective is to discover proteins that bind to AQP2 in a manner that is dependent on vasopressin-mediated changes in AQP2 phosphorylation.

One productive approach for discovery of protein-protein interactions involving AQP2 has been yeast 2-hybrid screening [19,20]. However, the yeast 2-hybrid approach is, in its present format, incapable of demonstrating phosphorylation-dependent interactions. Recently, proteomic approaches have become practical with the advent of protein mass spectrometry and genome sequencing projects. Barile *et al.* immunoisolated AQP2 bearing-vesicles to profile proteins contained in the same vesicular fraction as AQP2 [25]. Noda *et al.* used protein mass spectrometry coupled with immunoprecipitation to identify proteins directly associated with AQP2 [21].

Here, we employed a bait peptide pull-down approach similar to that of Thelin *et al.* [26], who investigated binding partners for CFTR and to that of McFarland *et al.* [27], who investigated binding partners for the differentially phosphorylated COOH-terminus of α-synuclein. We anticipated that finding binding partners with differential selectivities to these phosphorylated forms would have implications for their potential roles in AQP2 trafficking. Moreover, AQP2 binding partners could be involved in either endocytosis or exocytosis depending, in part, on their cellular localization. Here we used pull-downs with synthetic AQP2 COOH-terminal peptides and phosphopeptides to identify differentially bound proteins. As Ser-256 is the only known phosphorylation site in AQP2 directly phosphorylated by PKA and because this site has been demonstrated to be critical to regulation of AQP2 trafficking, we focused mainly on Ser-256 phosphorylated AQP2. We also included a Ser-261 phosphorylated peptide in our analysis since this site and the Ser-256 site have been demonstrated to be reciprocally regulated by vasopressin [10,28].

METHODS

Antibodies

Rabbit IgG directed against the AQP2 COOH-terminus was used as previously described [12]. Affinity purified rabbit IgG directed against NaPi-2 was used as a negative control for immunoprecipitation experiments because this protein is not expressed in the rat inner medulla [29,30]. Commercially available primary antibodies for immunoblotting are summarized in

Supplementary Methods. Fluorescent secondary antibodies against rabbit, mouse, goat, and chicken were purchased from Li-cor (Lincoln, NE) and Rockland (Gilbertsville, PA). HRP-conjugated TrueBlot anti-rabbit antibodies were purchased from eBioscience (San Diego, CA) for development of selected post-immunoprecipitation immunoblots.

Peptides and Proteins

Three biotinylated AQP2 COOH-terminal peptides were synthesized by AnaSpec (San Jose, CA). All had the following amino acid sequence: Biotin-LC-CEPDTDWEEREVRRRQSVELHSP QSLPRGSKA. One was phosphorylated at Ser-256 ("pS256 peptide"), one was phosphorylated at Ser-261 ("pS261 peptide") and one was unphosphorylated. ("nonphospho-peptide"). The sequence of each peptide was verified by mass spectrometry. Equality of the peptides concentrations was confirmed by dot blot analysis using fluorescently-conjugated streptavidin (IRDye 800, Rockland) to detect the biotinylated COOH-termini (see Supplementary Figure 2).

Circular Dichroism of Phosphopeptides

Circular dichroism was performed using a Jasco J-715 spectropolarimeter. Three sets of biotinylated peptide samples (non-phospho, pS256, and pS261) were prepared in 1X PBS. Samples were scanned from 200 to 260 nm with a band width of 0.5 nm, response time of 0.5 sec at a scanning speed of 50 nm/minute in a 0.2 cm cell with 10 accumulations per sample.

Animal studies

Pathogen-free male Sprague-Dawley rats (Taconic Farms, Germantown, NY) weighing 200 −250 g were maintained on an autoclaved pelleted rodent chow (413110−75−56, Zeigler Bros., Gardners, PA) and ad libitum drinking water. All experiments were conducted in accord with an animal protocol approved by the Animal Care and Use Committee of the National Heart, Lung, and Blood Institute (ACUC protocol number H-0110).

For AQP2 COOH-terminal peptide pull-downs, rats were provided sucrose water (250 mosm/kg) for two days in order to induce drinking to reduce baseline vasopressin levels. The urinary osmolality was 387 ± 485 (SD) mosm/kg (N=26). For all other experiments, rats were provided with *ad libitum* water. Inner medullary collecting duct (IMCD) tubule isolation from rat kidneys has been described previously [8,31].

Pull-Downs Using Biotinylated AQP2 COOH-Terminal Peptides

Pooled IMCD tubules from 4 rats (1−2 mg of total protein) were homogenized using a Potter-Elvehjem homogenizer (10 cycles, 15 second pulses) in "cytosolic buffer". Cytosolic buffer was designed to mimic intracellular osmolality, pH, and divalent cation concentrations. This buffer consisted of 180 mM Tris HCl, 2×10^{-4} mM Ca^{2+}, 0.8 mM Mg^{2+}, 1X phosphatase inhibitor cocktail (HALT, Pierce), protease inhibitor tablets (Complete Mini, Roche), and dithiothreitol (0.5 mg/ml), and was titrated to pH 7.2. Final osmolality was approximately 330 mosmol/kgH_2O. Homogenates were then spun at 200,000 X g for 1 h at 4°C. Supernatants ("cytosol") were saved and diluted approximately five to eight-fold in cytosolic buffer with detergents (1% Triton X-100, 0.1% SDS, and 0.5% sodium deoxycholate). This material was evenly divided into individual sample tubes (300 − 500 μg of protein per tube). To these tubes, either biotin (no peptide control), biotinylated nonphosphorylated AQP2 COOH-terminal peptide, pS256 peptide, or pS261 peptide was added in equimolar amounts (5 − 12 nmol depending on experiment). After vortexing, tubes were incubated overnight at room temperature with gentle agitation.

The following day, MyOne Streptavidin C1 Dynabeads (Invitrogen) that were pre-washed in cytosolic buffer (with detergents) were added to each tube in a ratio of 1 μg peptide/10 μl Dynabeads, or an approximately 1:1 ratio of biotin to streptavidin. Samples were incubated at room temperature with gentle rocking and periodic vortexing for two hours. Samples were washed four times with 500 μl cytosolic buffer with detergents. Samples were eluted in 1X Laemmli Buffer (1.5% SDS, 50 mM Tris (pH 6.8), and 6% glycerol).

Separation by 1-D SDS-PAGE and Trypsinization

Eluted samples from AQP2 COOH-terminal peptide pull-downs were run on 4−20% SDS-PAGE gels (Biorad, Hercules, CA) and stained with Coomassie blue. Entire lanes corresponding to eluates from each AQP2 COOH-terminal peptide were cut in parallel fashion, washed, reduced, alkylated, and trypsin-digested as described previously [32] and in detail in Supplementary Materials and Methods.

LC-MS/MS Protein Identification and Analysis

LC-MS/MS was performed on an LTQ tandem mass spectrometer (MS/MS, Thermo Electron Corp., San Jose, CA) via a nanoelectrospray ion source as described previously [33]. The spectra with a total ion current greater than 10,000 were used to search for matches to peptides in a concatenated RefSeq database using Bioworks software (Version 3.1, Thermo Electron Corp.) based on the Sequest algorithm. The concatenated “target/decoy” database was composed of forward protein sequences and reversed protein sequences derived from the NCBI using in-house software. Filtering parameters were set to achieve a desired false discovery rate of < 2% for individual peptides. All protein identifications in this study were based on multiple peptide matches.

Quantification of Mass Spectra

Spectral counting was used to test for differential abundances of proteins in AQP2 COOH-terminal peptide pull-down eluates. Proteins of interest were further analyzed for relative quantification by label-free quantification using QUOIL software, which calculated the ratios of the areas of the reconstructed peptide LC elution profiles from multiple samples [34]. The peptide mass tolerance was set to 0.5 Da. The minimal signal-to-noise threshold was set at 1.5 fold.

Immunoblotting

Samples in Laemmli buffer with DTT were heated to 65°C for 10 minutes; samples which contained Triton X-100 prior to addition of Laemmli buffer were heated at 37°C for 10 minutes. All samples were run on Criterion Tris-HCl polyacrylamide gels (Biorad). Transfers were performed at constant current (0.25 mAmp) for 1 hour in Fairbanks buffer. All membranes were blocked for at least one hour at room temperature using a proprietary blocking solution (Li-Cor Odyssey block). Primary antibody incubation was performed in Odyssey block with 0.1% Tween and 1.5 mM sodium azide overnight with rocking. Secondary incubation was performed in the same buffer but incubated for one hour at room temperature. Immunoblots were scanned and band density quantified using the Li-cor Odyssey fluorescence system. Co-immunoprecipitation immunoblots for annexin II, PP1c, and BiP were developed on Kodak X-AR film.

Immunoprecipitation of AQP2 from Native IMCD

Cells were incubated with 10^{-9} M dDAVP for 20 minutes in bicarbonate solution (pH 7.4) under 5% CO_2 for co-immunoprecipitation of BiP [8]. Isolated cells were lysed by Potter-Elvehjem homogenization in the presence of 0.1% Triton X-100, 0.01% SDS, and 0.05% sodium deoxycholate in cytosolic buffer. Total protein was measured in homogenates using

the BCA assay, and 100 μg total protein was used per sample. Enough DTT was added to achieve a concentration of 0.5 μg/ml. AQP2 was immunoprecipitated using a rabbit IgG antibody directed against a region of the COOH-terminus of AQP2, upstream from the polyphosphorylated region [12]. An affinity purified rabbit IgG directed against the proximal tubule sodium-phosphate co-transporter 2 (NaPi-2) was used as a negative control, since this transporter is not expressed in native collecting duct cells. Antibodies were tested for specificity: anti-AQP2 but not anti-NaPi-2 pulled down AQP2; anti-NaPi-2 recognized no IMCD proteins on immunoblotting (data not shown).

For these immunoprecipitations, 100 μg total IMCD protein with 15 μg IgG (control or anti-AQP2) was incubated in 200 μl cytosolic buffer containing protease and phosphatase inhibitors and DTT as above in the presence of 200 μg Triton X-100, 20 μg SDS, and 100 μg sodium deoxycholate. The detergent amount was chosen based on the rule-of-thumb stating a requirement of approximately 2 mg nonionic detergent per 1 mg membrane protein for full solubilization [35]. Samples were incubated overnight at 4°C with end-over-end rocking. Each sample was added to 100 μl of pre-washed protein G-coated Dynabeads. Capture was performed by end-over-end rotation for 1 hour at 4°C. Dynabeads were then washed 4 times with 500 μl of the same solution. Elution was performed twice in 2X Laemmli buffer with 77 mg/ml DTT at 37°C for 30 minutes, and eluates were pooled. Eluates were then run on SDS-PAGE and subjected to immunoblotting for the various putative AQP2 binding partners.

Preparation of tissue for immunogold electron microscopy

Fixed tissue blocks from the kidney inner medulla were infiltrated with 2.3 M sucrose for 30 min, and frozen in liquid nitrogen. Frozen tissue blocks were subjected to cryosubstitution and Lowicryl HM20 embedding. Lowicryl sections of 80 nm were cut on a Reichert Ultracut S and were preincubated with 0.05 M Tris, pH 7.4, 0.1% Triton-X-100 (TBST) containing 0.1% sodium borohydride and 0.05M glycine followed by incubation with TBST containing 0.2% skimmed milk. Preincubation was followed by incubation with anti-BiP rabbit polyclonal antibody (1:250, Abcam ab21685). Labeling was visualized with goat anti-rabbit IgG conjugated to colloidal gold particles. Grids were stained with uranyl acetate for 10 min and with lead citrate for 5 s.

Immunolabeling of kidney sections and confocal laser scanning microscopy

This technique has been described in detail previously [36]. Primary antibodies used were BiP (1:1000, Abcam ab21685); protein phosphatase 1 catalytic subunit, beta isoform (1:1000, Abcam, ab53315); annexin II (1:2000, Santa Cruz) and chicken anti-AQP2 (1:5000 dilution). A Leica TCS SL (SP2) laser confocal microscope and Leica Confocal Software was used for imaging of the kidney tissue sections. Images were taken using a HCX PL APO 63x oil immersion objective lens.

Statistical Analysis

Statistical analysis was conducted using InStat3 (Graphpad Software, La Jolla, CA). For immunoblot confirmation of mass spectrometric results, ANOVA analysis was performed with Bonferroni comparisons of multiple data sets.

RESULTS

Circular Dichroism

Figure 1 shows circular dichroism spectroscopic analysis of the biotinylated AQP2 COOH-terminal peptides used in this study. Peptides were carefully weighed to assure equal concentrations. The voltage graph in the bottom panel showing identical, overlapping curves

for each of the three AQP2 COOH-terminal peptides, indicating that their concentrations were virtually identical. The CD spectroscopic tracings for the peptides are non-superimposable, indicating a difference in secondary structure. The CD spectroscopic curves shown represent the mean ± SEM for a large number of overlapping points for three measurements per peptide. Between 220 and 224 nm, the nonphosphorylated peptide appears most alpha helical, the pS256 peptide appears least alpha helical, and the pS261 peptide is in between. These results suggest that each of the synthetic peptides used for pull-downs has a unique secondary structure.

Mass Spectrometric Analyses of AQP2 COOH-Terminal Peptide Pull-Downs

Proteins that were pulled down from the cytosol using AQP2 COOH-terminal peptides (either nonphosphorylated, phosphorylated at S256, or phosphorylated at S261) were identified by LC-MS/MS. Table 1 shows proteins that displayed differential binding relative to the "no peptide" controls based on overall spectral count from four separate trials ("experiment number 1−4"). (Trials in which the AQP2-pS261 peptide was not included are designated with an "x" in the pS261 column in Table 1.) We identified seven proteins that bound selectively to either the non-phosphorylated peptide or the pS256 peptide: 1) heat shock cognate 70 (also known as hsp70 isoform 8); 2) heat shock protein 70 (two different isoforms, namely hsp70 isoform 1 and hsp70 isoform 2); 3) BiP (also known as Grp78 or hsp70 isoform 5); 4) annexin II; 5) protein phosphatase 1 catalytic subunit; 6) GDP dissociation inhibitor 2 (GDI-2); and 7) ras-related nuclear protein (RAN). The unique RefSeq identifiers for these proteins are included in Table 1, allowing the reader to retrieve sequence and annotation information. Among the seven proteins identified, BiP bound selectively to the pS256 AQP2 COOH-terminal peptide, while the others bound selectively to the nonphosphorylated peptide. Furthermore, hsc70 bound selectively both to the nonphosphorylated and the pS261 peptides relative to the pS256 peptide. Supplementary Table 1 lists the unique peptides identified for each of the seven proteins in each experiment.

To confirm and quantify the semi-quantitative results described in Table 1, we carried out label-free quantification of reconstructed ion chromatograms from the spectra generated for Table 1 [34]. Reconstructed MS1 ion chromatograms for selected peptides are shown in Figures 2A-G. Table 2 shows formal quantification of proteins that displayed differential binding relative to the "no peptide" controls based on average area under the reconstructed ion chromatograms for all peptides of a given protein. Proteins that were identified as having statistically significant binding differences in AQP2 phosphorylated "bait" peptides (pS256 or pS261) versus the nonphosphorylated AQP2 "bait" peptide are indicated.

Confirmation by Immunoblotting

To confirm results obtained by mass spectrometry, the same eluates were evaluated by immunoblotting (Figure 3A-C). Two positive controls were used: 1) whole IMCD homogenate (to demonstrate the presence of each of the seven identified proteins in the rat IMCD) and 2) pre-pull-down cytosol. Each of the seven proteins identified by mass spectrometry was present in this cytosolic fraction. The immunoblots confirmed that hsc70, hsp70, annexin II, PP1c, GDI-2, and RAN all bound more to the nonphosphorylated peptide than to the phosphorylated peptides. In contrast, co-immunoprecipitated BiP was greatest in the eluate from the pS256 peptide, slightly visible in the eluate from the nonphosphorylated peptide, and undetectable in the eluate from pS261 peptide.

Figures 3B and 3C show quantified band densities. Statistically significantly greater abundance ($p<0.05$ by ANOVA Bonferroni comparison across multiple samples) was demonstrated in the eluates corresponding to the nonphosphorylated COOH-terminal peptide pull-downs for hsc70 (n=5), hsp70 (n=3), annexin II (n=4), PP1c (n=4), and RAN (n=4). There was also statistically significantly greater abundance of hsc70 in the eluates corresponding to the pS261 peptide

compared to those of pS256. Again, BiP (n=3) strongly and selectively bound to the pS256 peptide (Figure 3C).

Given the presence of PP1c, we asked whether another common S/T phosphatase, PP2Ac, was also present in pull-down eluates. Immunoblotting detected this protein in positive controls but not in any of the eluates corresponding to the AQP2 COOH-terminal peptides (Supplementary Figure 6). This suggests a specific association between PP1c but not PP2Ac and the COOH-terminus of AQP2.

Co-immunoprecipitation of AQP2 binding partners

To test whether proteins that bound *in vitro* AQP2 COOH-terminal peptides also bound to native AQP2, immunoprecipitation was performed using an anti-AQP2 antibody followed by immunoblotting for specific, putative binding partners (Figure 4). Three out of the seven proteins that bound *in vitro* were also found to co-immunoprecipitate with native AQP2. (Due to standard technical limitations, we could not confirm that the other four proteins bind *in vivo*.) Annexin II (n=4) and PP1c (n=4) were present in eluates, suggesting an association between these proteins and native AQP2 in native rat IMCD cells. To analyze whether BiP was present in eluates corresponding to immunoisolated AQP2, rat IMCD cells were first treated with dDAVP to maximize the amount of pS256-AQP2 in the cells. BiP was present in these eluates (n=2). This finding further demonstrated a previously unknown interaction between BiP and native AQP2. To confirm the interaction between AQP2 and these potential binding partners using an orthogonal system, we also co-immunoprecipitated BiP, PP1c, and annexin II using an N-terminal AQP2 antibody in MDCK cells stably transfected with wildtype AQP2 (Supplementary Figure 7). In cells stably transfected with an AQP2 construct containing an S256A mutation, co-immunoprecipitation of these 3 proteins was significantly reduced. These proteins were not present in eluates when non-related immune serum was used for the immunoprecipitation (data not shown).

Immunogold electron microscopy of BiP in normal rat kidney

BiP is known to be an endoplasmic reticulum resident protein, but also has been demonstrated to be present throughout the cytoplasm in other studies [37-43]. We performed immunogold electron microscopy in order to definitively address whether BiP is also located outside the ER in IMCD cells. In inner medulla, BiP localized both intracellularly and to the apical plasma membrane of collecting duct principal cells (Figure 5). A part of the intracellular localization was in a distribution consistent with its presence in the ER.

Co-localization of AQP2 and binding partners by confocal immunofluorescence microscopy

We carried out immunofluorescence immunocytochemistry in order to localize the AQP2 binding partners BiP, PP1c, and annexin II. BiP partially co-localized with AQP2 in both cytoplasm and at the apical region of IMCD principal cells (Figure 6A-H). A cytoplasmic distribution was found for PP1c in IMCD (Figure 6I), with a more apical co-localization with AQP2 in cortical collecting duct (Figure 6M). Annexin II was also localized to collecting ducts along with AQP2 (Figure 6N). In the initial IMCD (Figure 6O), annexin II and AQP2, partially co-localized at the apical plasma membrane.

DISCUSSION

In this study, we aimed to identify binding partners to the differentially-phosphorylated forms of the AQP2 COOH-terminus, the portion of the AQP2 molecule that has been implicated in the regulation of trafficking to the apical plasma membrane [2,5,6]. We used protein mass spectrometry as a tool to establish binding partners' identities and relative abundances in the eluates of a cytosolic pull-down experiment using synthetic AQP2 COOH-terminal peptides.

Mass spectrometry was used as an initial screening tool, followed by confirmation by semi-quantitative immunoblotting and evaluation of identified interactions with native AQP2 by coimmunoprecipitation. Evaluation of mass spectra and subsequent verification by immunoblotting demonstrated the associations between hsp70/hsc70 and AQP2 shown by Lu *et al* [19] Our studies further verified and characterized the association between annexin II and AQP2 previously demonstrated from mass spectrometric analysis of AQP2 immunoprecipitates [44].

Other proteins that have been shown previously to interact with AQP2, namely SPA-1 [17] and MAL [20], were not identified in the present study. SPA-1 is a RapGAP [17]. According to the IMCD transcriptome database (http://dir.nhlbi.nih.gov/papers/lkem/imcdtr), the abundance of SPA-1 mRNA is very low in the IMCD [45], suggesting that the protein abundance may be low as well, limiting our ability to detect it. MAL is an integral membrane protein. Our pull-downs utilized only the cytosolic fraction of IMCD cells for incubation with AQP2 COOH-terminal peptides. Thus, we would not expect to have identified MAL in these experiments.

Our studies, then, yielded seven candidate binding partners to the AQP2 COOH-terminus as demonstrated quantitatively by protein mass spectrometry and by immunoblotting of pull-downs: hsc70, hsp70 (isoforms 1 and 2), BiP (Grp78, or hsp70 isoform 5), annexin II, PP1c, GDI-2, and RAN. With the notable exception of BiP, which was most abundant in the eluates corresponding to the pS256 AQP2 COOH-terminal peptide pull-downs, the other candidate binding partners showed a preference for the nonphosphorylated peptide. Interestingly, hsc70 showed a small but statistically significant preference for the nonphosphorylated and pS261 COOH-terminal AQP2 tail peptides over the pS256 peptide.

Studies using circular dichroism, a spectroscopic technique capable of elucidating peptide and protein secondary structure, demonstrated that the nonphosphorylated form of the AQP2 COOH-terminus appeared most alpha−helical; phosphorylation at Ser-256 significantly altered this conformation, and phosphorylation at Ser-261 caused a less pronounced change. These findings are consistent with the hypothesis that a charge effect from phosphorylation is not the sole mediator of binding partner selectivity for the differentially phosphorylated AQP2 COOH-terminus. Thus, we may partially explain slight changes in binding partner selectivities to the AQP2 COOH-terminus by alteration of secondary structure due to phosphorylation. In the remainder of this discussion, we describe potential physiologic consequences for these demonstrated protein-protein interactions.

The direct interaction of hsp70 and hsc70 with AQP2 was initially characterized by Lu *et al* [19]. Our findings are consistent with their GST and native protein pull-down studies. Moreover, we were able to demonstrate different selectivities of hsp70 and hsc70 for the various *in vitro* phosphophorylated AQP2 COOH-terminal peptides. Our *in vitro* data suggested that hsc70 and hsp70 interact selectively with AQP2 that is not phosphorylated at Ser-256, which would be expected to be more abundant in the absence of vasopressin. Lu *et al*. showed that functional knockdown of hsc70 induced membrane accumulation of AQP2, demonstrating potential involvement of hsc70 in clathrin-mediated endocytosis of AQP2 [19].

BiP is a unique member of the hsp70 family, whose primary function is believed to be in the quality control mechanism in the ER. Its unique KDEL sequence is known to be an ER localization signal [46]. However, a number of studies have shown BiP localization at the plasma membrane and cytosol in a variety of cell types [37-43]. We have confirmed these conclusions in collecting duct cells using immunogold EM and confocal immunofluorescence microscopy. BiP appeared in our cytosolic fractions of IMCD cell homogenates, despite stringent ultracentrifugation prior to the AQP2 COOH-terminal peptide pull-down experiments. We further confirmed an association between native AQP2 and BiP by immunoprecipitation of

AQP2 from native IMCD cells and subsequent immunoblotting for BiP. BiP abundance has been shown to decrease in animals subjected to long-term vasopressin escape, a condition in which pS256-AQP2 theoretically decreases compared to control animals [47]. In contrast, BiP abundance has been shown to increase in the IMCD after long-term lithium treatment [48]. Our finding that BiP preferentially binds pS256 AQP2 COOH-terminal peptides suggests a trafficking role for this protein or possibly a counter-regulatory role in hsc70/hsp70-mediated endocytosis of AQP2. Alternatively, BiP binding to pS256 may alter the conformation of the C-terminal tail of AQP2, thereby promoting the association of kinases that phosphorylate AQP2 at neighboring sites. This could potentially explain the dependence of phosphorylation at S264 and S269 on prior phosphorylation at S256 as demonstrated by Hoffert *et al.* [12].

Several studies have suggested an association between annexin II and AQP2 [21,22]. Annexins have been a subject of interest in AQP2 trafficking since Hill *et al.* identified an association—though not a functional one—between annexin IV and AQP2 [49]. Barile *et al.* found that immunoisolated AQP2-bearing vesicles contained annexins I, II, IV, and V [25]. Furthermore, Noda *et al.* identified annexin II as part of a "multiprotein 'motor' complex" associated with immunoprecipitated AQP2 [21]. We found preferential binding of annexin II to the nonphosphorylated AQP2 COOH-terminal peptide. A direct association was confirmed by co-immunoprecipitation of annexin II with an antibody against AQP2. Since annexin II has been shown to be involved in both endocytosis and exocytosis, it is possible that this protein functions in both processes in the collecting duct [50]. Finally, a recent study by Tamma *et al.* demonstrates that inhibition of annexin II impairs water permeability in cultured cells [22].

PKA has been demonstrated to bear responsibility for phosphorylation of Ser-256. To our knowledge, until the present study, no phosphatases have been proven to associate directly with the COOH-terminus of AQP2. A study by Valenti *et al.* suggested a functional interaction between AQP2 and either PP2A or PP1 [51]. That particular study found that the phosphatase inhibitor okadaic acid, at concentrations high enough to inhibit both phosphatases, increased osmotic water permeability and increased AQP2 trafficking to the plasma membrane. These findings, taken together with our findings that PP1c, but not PP2Ac, preferentially binds the nonphosphorylated AQP2 COOH-terminus *in vitro* (by peptide pulldown and immunoblotting), suggests the hypothesis that PP1 may play a role in regulation of the phosphorylation state of the COOH-terminus of AQP2 in the unstimulated state.

The significance of the *in vitro* association between the AQP2 COOH-terminus and both GDI-2 and RAN remains unclear. GDP dissociation inhibitors such as GDI-2 maintain small GTPases in their inactive state, preventing their insertion into membranes [52,53]. This finding suggests a potential role of Ras-like GTPase trafficking in regulation of AQP2. Unlike GDI-2, RAN is primarily known to function in nuclear-cytoplasmic trafficking (possibly bi-directionally) and in nuclear functions in mitosis, but it is also present in the cytosol [54,55]. In a recent proteomics study by Nielsen *et al.*, RAN expression was increased in the IMCD after two weeks of lithium treatment [48]. However, no clear connection has been established between changes in RAN expression and lithium-induced down-regulation of AQP2.

In summary, our studies have used mass spectrometry to identify seven potential binding partners to the AQP2 COOH-terminus in rat IMCD cells. These proteins have differential selectivities for phosphorylated versus nonphosphorylated AQP2 COOH-terminal, synthetic peptides *in vitro*. Furthermore, using an antibody to AQP2, we have been able to co-immunoprecipitate three of the protein binding partners (i.e. annexin II, PP1c, and BiP) from native IMCD cells as well as from a stably-transfected kidney cell line. We also demonstrated, through immunofluorescence microscopy, that these proteins co-localize with endogenous AQP2 in native rat collecting duct.

Supplementary Material

Refer to Web version on PubMed Central for supplementary material.

ACKNOWLEDGMENTS

We are grateful to Grzegorz Piszczek, of the National Heart, Lung, and Blood Institute Laboratory of Biochemistry for his assistance with CD spectrometry. Protein mass spectrometry was carried out in the Proteomics Core Facility of the NHLBI Division of Intramural Research. We thank Else-Merete Løcke for expert technical assistance in immunolabeling experiments. Nicholas Zwang is supported by Howard Hughes Medical Institute-National Institutes of Health Research Scholars Program. Robert A. Fenton is supported by a Marie Curie Intra-European Fellowship and the Danish Medical Research Foundation. The Water and Salt Research Center at the University of Aarhus was established and supported by the Danish National Research Foundation (Danmarks Grundforskningsfond). This work was also supported in part by the intramural budget of the National Heart, Lung, and Blood Institute (Z01-HL-01285-KE).

References

1. Nielsen S, Chou CL, Marples D, Christensen EI, Kishore BK, Knepper MA. Vasopressin increases water permeability of kidney collecting duct by inducing translocation of aquaporin-CD water channels to plasma membrane. Proc. Natl. Acad. Sci. U. S. A 1995;92(4):1013–1017. [PubMed: 7532304]
2. Brown D. The ins and outs of aquaporin-2 trafficking. Am. J. Physiol Renal Physiol 2003;284(5):F893–F901. [PubMed: 12676734]
3. Knepper MA, Nielsen S. Kinetic model of water and urea permeability regulation by vasopressin in collecting duct. Am. J. Physiol 1993;265(2 Pt 2):F214–F224. [PubMed: 8396343]
4. Nielsen S, Knepper MA. Vasopressin activates collecting duct urea transporters and water channels by distinct physical processes. Am. J. Physiol 1993;265(2 Pt 2):F204–F213. [PubMed: 8396342]
5. Boone M, Deen PM. Physiology and pathophysiology of the vasopressin-regulated renal water reabsorption. Pflugers Arch 2008;456:1005–1024. [PubMed: 18431594]
6. Nielsen S, Frokiaer J, Marples D, Kwon TH, Agre P, Knepper MA. Aquaporins in the kidney: from molecules to medicine. Physiol Rev 2002;82(1):205–244. [PubMed: 11773613]
7. Star RA, Nonoguchi H, Balaban R, Knepper MA. Calcium and cyclic adenosine monophosphate as second messengers for vasopressin in the rat inner medullary collecting duct. J. Clin. Invest 1988;81(6):1879–1888. [PubMed: 2838523]
8. Chou CL, Yip KP, Michea L, Kador K, Ferraris JD, Wade JB, Knepper MA. Regulation of aquaporin-2 trafficking by vasopressin in the renal collecting duct. Roles of ryanodine-sensitive Ca2+ stores and calmodulin. J. Biol. Chem 2000;275(47):36839–36846. [PubMed: 10973964]
9. Chou CL, Christensen BM, Frische S, Vorum H, Desai RA, Hoffert JD, de LP, Nielsen S, Knepper MA. Non-muscle Myosin II and Myosin Light Chain Kinase Are Downstream Targets for Vasopressin Signaling in the Renal Collecting Duct. J. Biol. Chem 2004;279(47):49026–49035. [PubMed: 15347643]
10. Hoffert JD, Pisitkun T, Wang G, Shen RF, Knepper MA. Quantitative phosphoproteomics of vasopressin-sensitive renal cells: regulation of aquaporin-2 phosphorylation at two sites. Proc. Natl. Acad. Sci. U. S. A 2006;103(18):7159–7164. [PubMed: 16641100]
11. Fenton RA, Moeller HB, Hoffert JD, Yu MJ, Nielsen S, Knepper MA. Acute regulation of aquaporin-2 phosphorylation at Ser-264 by vasopressin. Proc. Natl. Acad. Sci. U. S. A 2008;105(8):3134–3139. [PubMed: 18287043]
12. Hoffert JD, Fenton RA, Moeller HB, Simons B, Tchapyjnikov D, McDill BW, Yu MJ, Pistikun T, Chen F, Knepper MA. Vasopressin-stimulated increase in phosphorylation at ser-269 potentiates plasma membrane retention of aquaporin-2. J. Biol. Chem 2008;283:24617–24627. [PubMed: 18606813]
13. Katsura T, Gustafson CE, Ausiello DA, Brown D. Protein kinase A phosphorylation is involved in regulated exocytosis of aquaporin-2 in transfected LLC-PK1 cells. Am. J. Physiol 1997;272(6 Pt 2):F817–F822. [PubMed: 9227644]

14. Fushimi K, Sasaki S, Marumo F. Phosphorylation of serine 256 is required for cAMP-dependent regulatory exocytosis of the aquaporin-2 water channel. J. Biol. Chem 1997;272(23):14800–14804. [PubMed: 9169447]
15. Kamsteeg EJ, Heijnen I, van Os CH, Deen PM. The subcellular localization of an aquaporin-2 tetramer depends on the stoichiometry of phosphorylated and nonphosphorylated monomers. J. Cell Biol 2000;151(4):919–930. [PubMed: 11076974]
16. Lu HJ, Matsuzaki T, Bouley R, Hasler U, Qin QH, Brown D. The phosphorylation state of serine 256 is dominant over that of serine 261 in the regulation of AQP2 trafficking in renal epithelial cells. Am. J. Physiol Renal Physiol 2008;295(1):F290–F294. [PubMed: 18434387]
17. Noda Y, Horikawa S, Furukawa T, Hirai K, Katayama Y, Asai T, Kuwahara M, Katagiri K, Kinashi T, Hattori M, Minato N, Sasaki S. Aquaporin-2 trafficking is regulated by PDZ-domain containing protein SPA-1. FEBS Lett 2004;568(1−3):139–145. [PubMed: 15196935]
18. Noda Y, Horikawa S, Katayama Y, Sasaki S. Water channel aquaporin-2 directly binds to actin. Biochem. Biophys. Res. Commun 2004;322(3):740–745. [PubMed: 15336526]
19. Lu HA, Sun TX, Matsuzaki T, Yi XH, Eswara J, Bouley R, McKee M, Brown D. Heat shock protein 70 interacts with aquaporin-2 and regulates its trafficking. J. Biol. Chem 2007;282(39):28721–28732. [PubMed: 17636261]
20. Kamsteeg EJ, Duffield AS, Konings IB, Spencer J, Pagel P, Deen PM, Caplan MJ. MAL decreases the internalization of the aquaporin-2 water channel. Proc. Natl. Acad. Sci. U. S. A 2007;104(42): 16696–16701. [PubMed: 17940053]
21. Noda Y, Horikawa S, Katayama Y, Sasaki S. Identification of a multiprotein “motor” complex binding to water channel aquaporin-2. Biochem. Biophys. Res. Commun 2005;330(4):1041–1047. [PubMed: 15823548]
22. Tamma G, Procino G, Mola MG, Svelto M, Valenti G. Functional involvement of Annexin-2 in cAMP induced AQP2 trafficking. Pflugers Arch 2008;456(4):729–736. [PubMed: 18389276]
23. Noda Y, Horikawa S, Kanda E, Yamashita M, Meng H, Eto K, Li Y, Kuwahara M, Hirai K, Pack C, Kinjo M, Okabe S, Sasaki S. Reciprocal interaction with G-actin and tropomyosin is essential for aquaporin-2 trafficking. J. Cell Biol 2008;182(3):587–601. [PubMed: 18678705]
24. Okutsu R, Rai T, Kikuchi A, Ohno M, Uchida K, Sasaki S, Uchida S. AKAP220 colocalizes with AQP2 in the inner medullary collecting ducts. Kidney Int 2008;74(11):1429–1433. [PubMed: 19008911]
25. Barile M, Pisitkun T, Yu MJ, Chou CL, Verbalis MJ, Shen RF, Knepper MA. Large scale protein identification in intracellular aquaporin-2 vesicles from renal inner medullary collecting duct. Mol. Cell Proteomics 2005;4(8):1095–1106. [PubMed: 15905145]
26. Thelin WR, Kesimer M, Tarran R, Kreda SM, Grubb BR, Sheehan JK, Stutts MJ, Milgram SL. The cystic fibrosis transmembrane conductance regulator is regulated by a direct interaction with the protein phosphatase 2A. J. Biol. Chem 2005;280(50):41512–41520. [PubMed: 16239222]
27. McFarland MA, Ellis CE, Markey SP, Nussbaum RL. Proteomic analysis identifies phosphorylation-dependent a-synuclein protein interactions. Mol. Cell Proteomics. 2008
28. Hoffert JD, Nielsen J, Yu MJ, Pisitkun T, Schleicher SM, Nielsen S, Knepper MA. Dynamics of aquaporin-2 serine-261 phosphorylation in response to short-term vasopressin treatment in collecting duct. Am. J. Physiol Renal Physiol 2007;292(2):F691–F700. [PubMed: 16985212]
29. Kim GH, Martin SW, Fernandez-Llama P, Masilamani S, Packer RK, Knepper MA. Long-term regulation of renal Na-dependent cotransporters and ENaC: response to altered acid-base intake. Am. J. Physiol Renal Physiol 2000;279(3):F459–F467. [PubMed: 10966925]
30. Turban S, Beutler KT, Morris RG, Masilamani S, Fenton RA, Knepper MA, Packer RK. Long-term regulation of proximal tubule acid-base transporter abundance by angiotensin II. Kidney Int 2006;70 (4):660–668. [PubMed: 16807546]
31. Stokes JB, Grupp C, Kinne RK. Purification of rat papillary collecting duct cells: functional and metabolic assessment. Am J Physiol 1987;253(2 Pt 2):F251–F262. [PubMed: 3303974]
32. Pisitkun T, Shen RF, Knepper MA. Identification and proteomic profiling of exosomes in human urine. Proc. Natl. Acad. Sci. U. S. A 2004;101(36):13368–13373. [PubMed: 15326289]

33. Yu MJ, Pisitkun T, Wang G, Aranda JF, Gonzales PA, Tchapyjnikov D, Shen RF, Alonso MA, Knepper MA. Large-scale quantitative LC-MS/MS analysis of detergent-resistant membrane proteins from rat renal collecting duct. Am. J. Physiol Cell Physiol. 2008
34. Wang G, Wu WW, Zeng W, Chou CL, Shen RF. Label-free protein quantification using LC-coupled ion trap or FT mass spectrometry: Reproducibility, linearity, and application with complex proteomes. J. Proteome. Res 2006;5(5):1214–1223. [PubMed: 16674111]
35. Scopes, RK. Protein Purification: Principles and Practice. Vol. 41. Springer Science + Business Media, Inc.; New York, NY: 1994. Ref Type: Generic
36. Fenton RA, Brond L, Nielsen S, Praetorius J. Cellular and subcellular distribution of the type-2 vasopressin receptor in the kidney. Am. J. Physiol Renal Physiol 2007;293(3):F748–F760. [PubMed: 17553938]
37. Shani G, Fischer WH, Justice NJ, Kelber JA, Vale W, Gray PC. GRP78 and Cripto form a complex at the cell surface and collaborate to inhibit transforming growth factor beta signaling and enhance cell growth. Mol. Cell Biol 2008;28(2):666–677. [PubMed: 17991893]
38. Delpino A, Castelli M. The 78 kDa glucose-regulated protein (GRP78/BIP) is expressed on the cell membrane, is released into cell culture medium and is also present in human peripheral circulation. Biosci. Rep 2002;22(3−4):407–420. [PubMed: 12516782]
39. Altmeyer A, Maki RG, Feldweg AM, Heike M, Protopopov VP, Masur SK, Srivastava PK. Tumor-specific cell surface expression of the-KDEL containing, endoplasmic reticular heat shock protein gp96. Int. J. Cancer 1996;69(4):340–349. [PubMed: 8797880]
40. Davidson DJ, Haskell C, Majest S, Kherzai A, Egan DA, Walter KA, Schneider A, Gubbins EF, Solomon L, Chen Z, Lesniewski R, Henkin J. Kringle 5 of human plasminogen induces apoptosis of endothelial and tumor cells through surface-expressed glucose-regulated protein 78. Cancer Res 2005;65(11):4663–4672. [PubMed: 15930284]
41. Xiao G, Chung TF, Pyun HY, Fine RE, Johnson RJ. KDEL proteins are found on the surface of NG108−15 cells. Brain Res. Mol. Brain Res 1999;72(2):121–128. [PubMed: 10529470]
42. Boilard M, Reyes-Moreno C, Lachance C, Massicotte L, Bailey JL, Sirard MA, Leclerc P. Localization of the chaperone proteins GRP78 and HSP60 on the luminal surface of bovine oviduct epithelial cells and their association with spermatozoa. Biol. Reprod 2004;71(6):1879–1889. [PubMed: 15286042]
43. Wiest DL, Bhandoola A, Punt J, Kreibich G, McKean D, Singer A. Incomplete endoplasmic reticulum (ER) retention in immature thymocytes as revealed by surface expression of “ER-resident” molecular chaperones. Proc. Natl. Acad. Sci. U. S. A 1997;94(5):1884–1889. [PubMed: 9050874]
44. Noda Y, Sasaki S. Regulation of aquaporin-2 trafficking and its binding protein complex. Biochim. Biophys. Acta 2006;1758(8):1117–1125. [PubMed: 16624255]
45. Uawithya P, Pisitkun T, Ruttenberg BE, Knepper MA. Transcriptional profiling of native inner medullary collecting duct cells from rat kidney. Physiol Genomics 2008;32(2):229–253. [PubMed: 17956998]
46. Daugaard M, Rohde M, Jaattela M. The heat shock protein 70 family: Highly homologous proteins with overlapping and distinct functions. FEBS Lett 2007;581(19):3702–3710. [PubMed: 17544402]
47. Hoorn EJ, Hoffert JD, Knepper MA. Combined proteomics and pathways analysis of collecting duct reveals a protein regulatory network activated in vasopressin escape. J. Am. Soc. Nephrol 2005;16 (10):2852–2863. [PubMed: 16079266]
48. Nielsen J, Hoffert JD, Knepper MA, Agre P, Nielsen S, Fenton RA. Proteomic analysis of lithium-induced nephrogenic diabetes insipidus: mechanisms for aquaporin 2 down-regulation and cellular proliferation. Proc. Natl. Acad. Sci. U. S. A 2008;105(9):3634–3639. [PubMed: 18296634]
49. Hill WG, Kaetzel MA, Kishore BK, Dedman JR, Zeidel ML. Annexin A4 reduces water and proton permeability of model membranes but does not alter aquaporin 2-mediated water transport in isolated endosomes. J. Gen. Physiol 2003;121(5):413–425. [PubMed: 12695484]
50. Gerke V, Creutz CE, Moss SE. Annexins: linking Ca2+ signalling to membrane dynamics. Nat. Rev. Mol. Cell Biol 2005;6(6):449–461. [PubMed: 15928709]
51. Valenti G, Procino G, Carmosino M, Frigeri A, Mannucci R, Nicoletti I, Svelto M. The phosphatase inhibitor okadaic acid induces AQP2 translocation independently from AQP2 phosphorylation in renal collecting duct cells. J. Cell Sci 2000;113(Pt 11):1985–1992. [PubMed: 10806109]

52. Olofsson B. Rho guanine dissociation inhibitors: pivotal molecules in cellular signalling. Cell Signal 1999;11(8):545–554. [PubMed: 10433515]

53. Dovas A, Couchman JR. RhoGDI: multiple functions in the regulation of Rho family GTPase activities. Biochem. J 2005;390(Pt 1):1–9. [PubMed: 16083425]

54. Joseph J. Ran at a glance. J. Cell Sci 2006;119(Pt 17):3481–3484. [PubMed: 16931595]

55. Dasso M. The Ran GTPase: theme and variations. Curr. Biol 2002;12(14):R502–R508. [PubMed: 12176353]

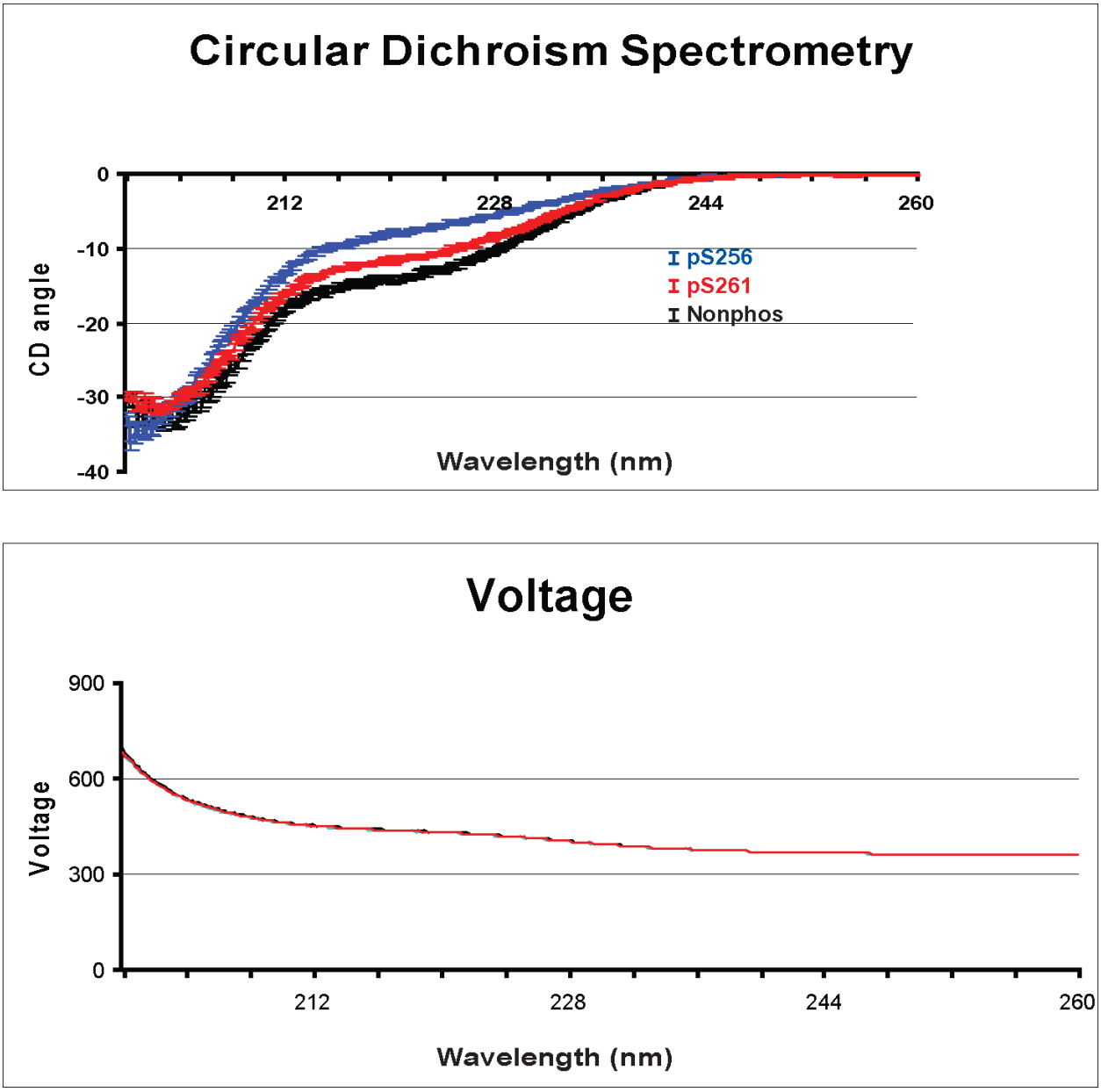

Figure 1. Circular dichroism spectrometry of AQP2 COOH-terminal peptides

Three different phosphorylated forms of the same biotinylated 32 amino acid peptide corresponding to the COOH-terminus of AQP2 (nonphos, pS256, and pS261) were subjected to circular dichroism spectrometry. Peptides were weighed and diluted to equal concentrations for analysis. Experiments were performed in triplicate. Top graph shows circular dichroism angle of deflection at wavelengths from 0 to 260 nm. Bottom graph shows superimposable voltage (V) curves for each peptide.

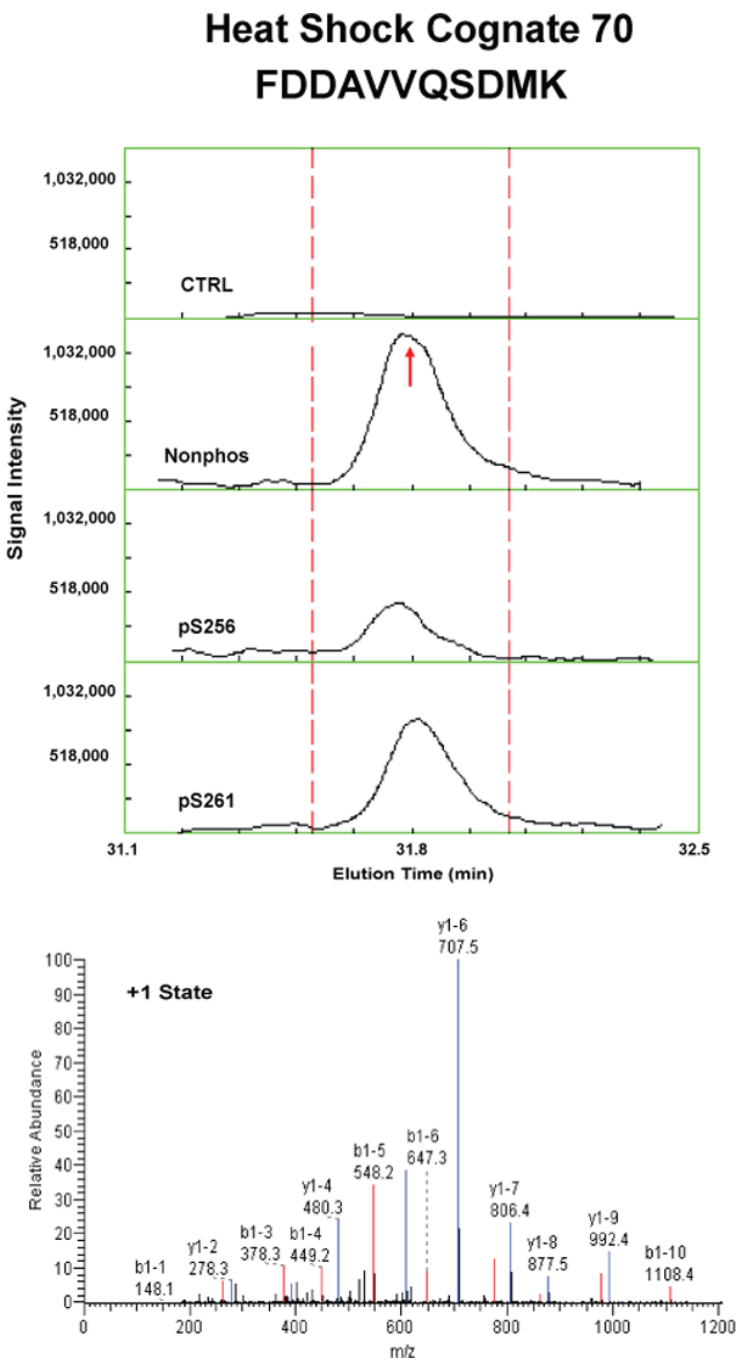

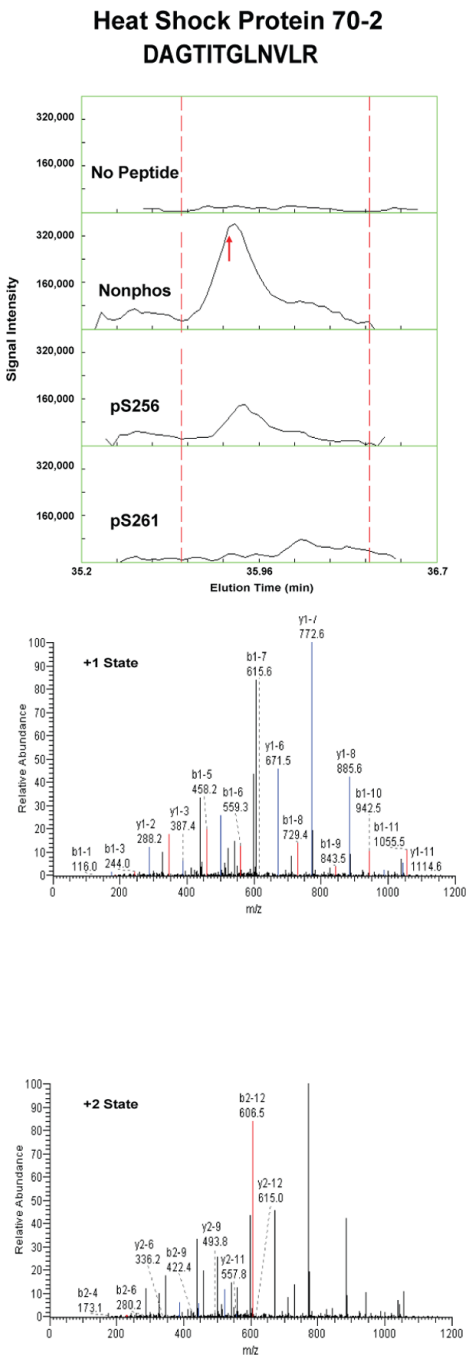

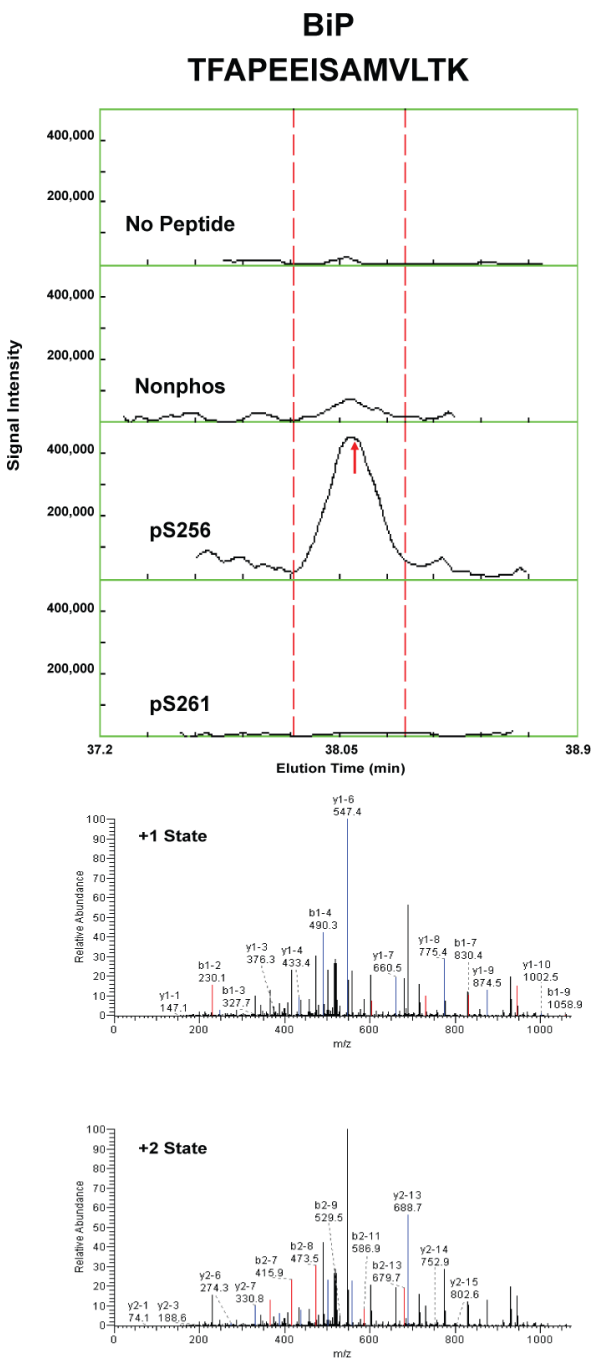

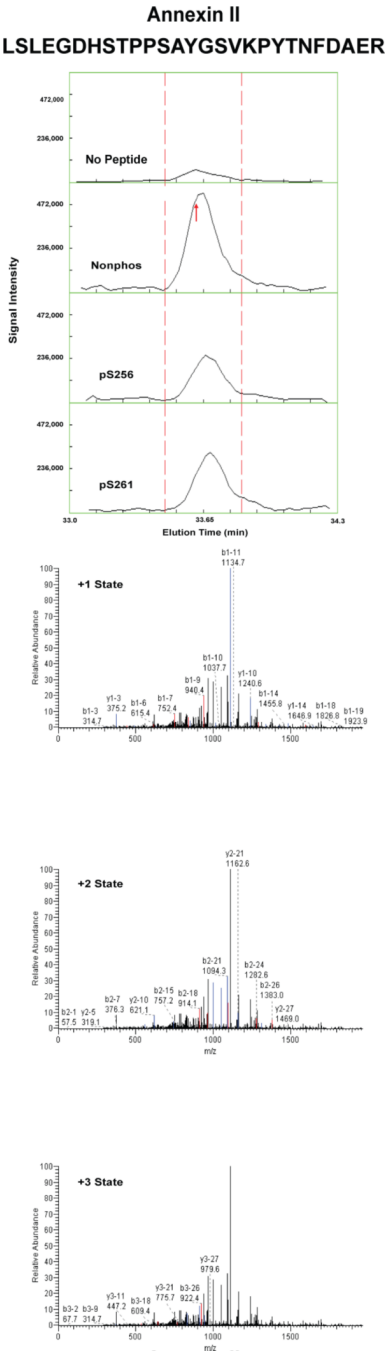

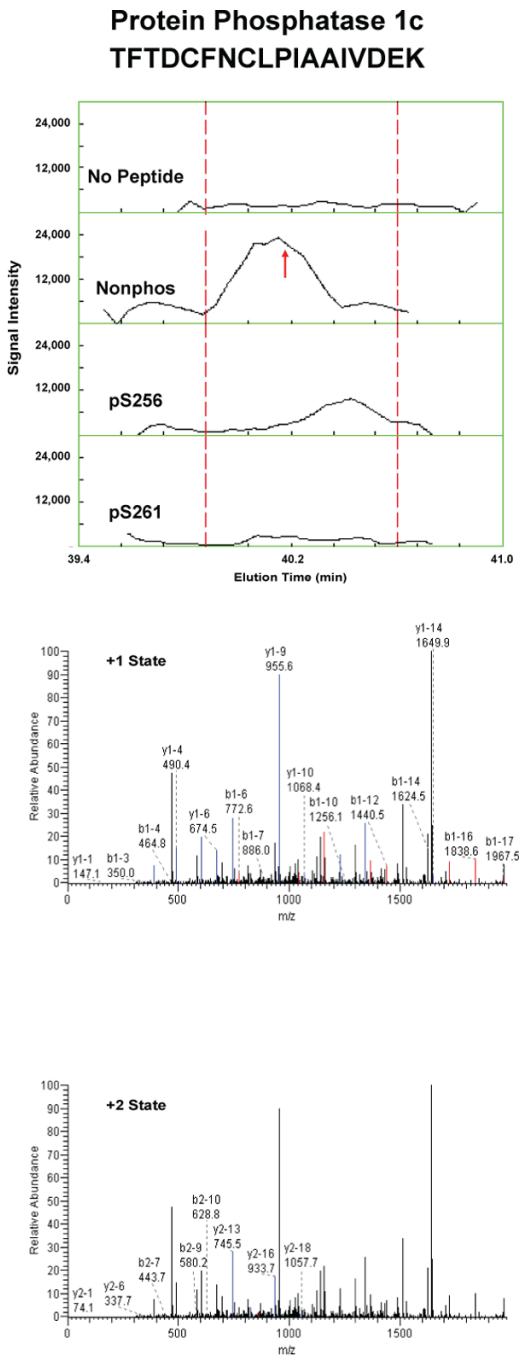

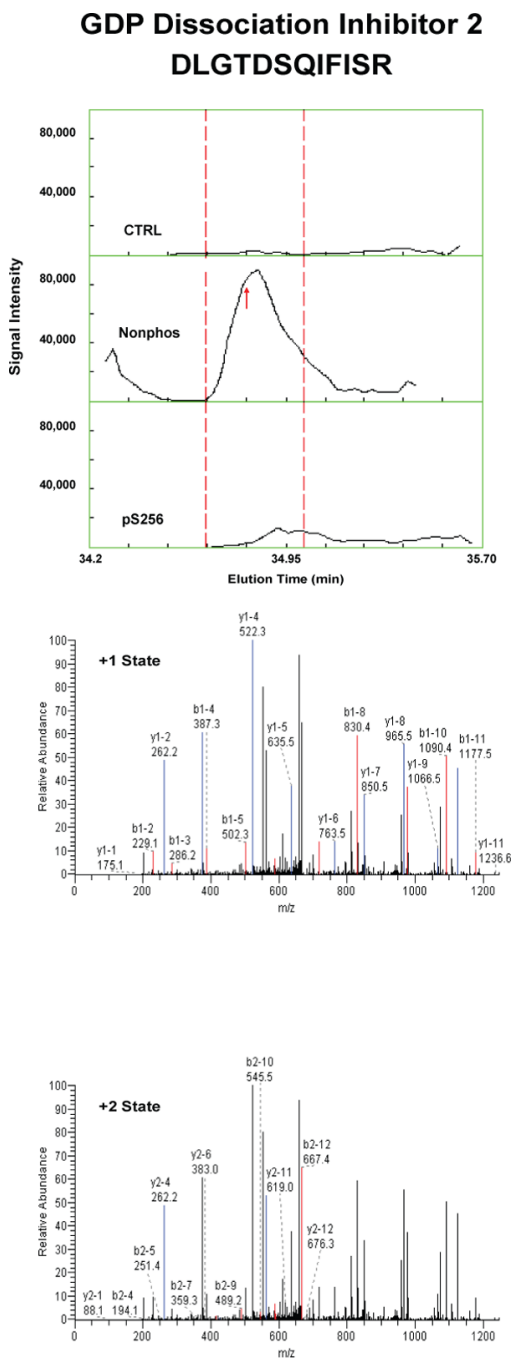

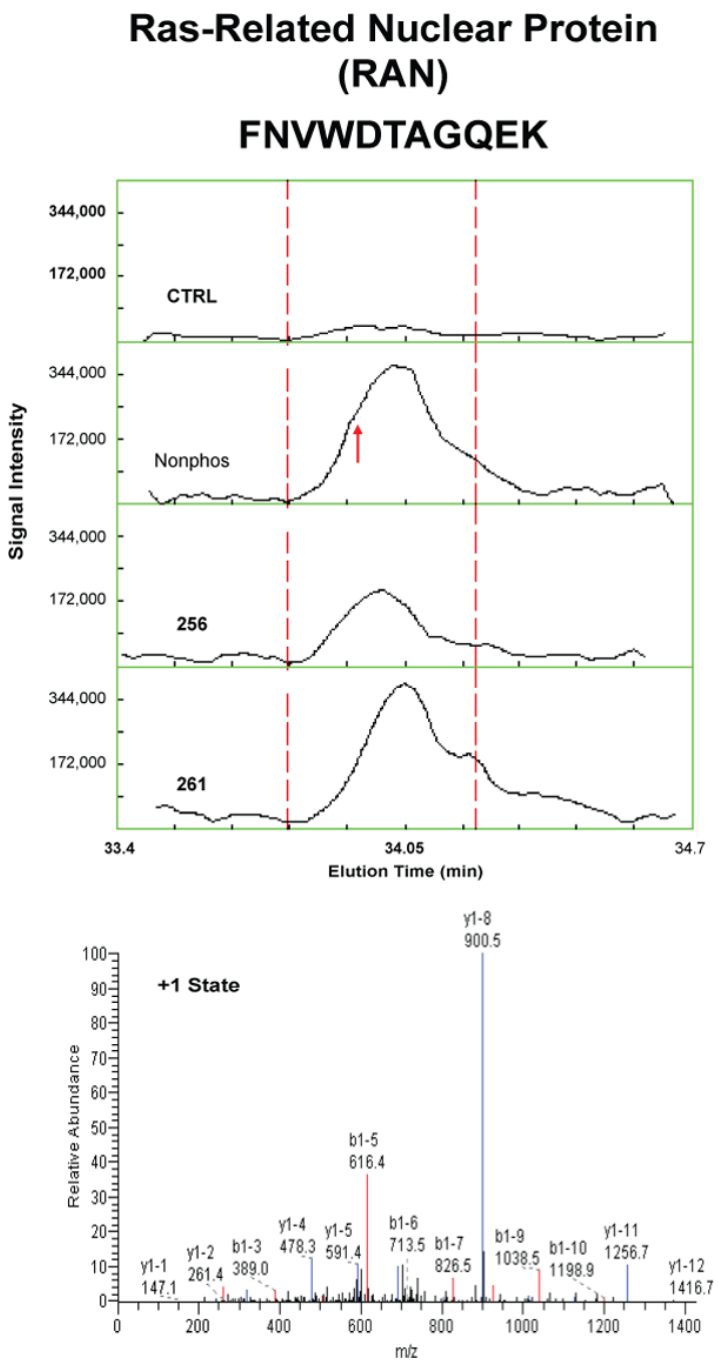

Figure 2. Mass spectra of peptides identified in eluates of AQP2 peptide pull-downs

Each figure shows a peptide sequence corresponding to one of seven proteins identified in the eluates from AQP2 peptide pull-downs subjected to mass spectrometry: heat shock cognate 70; heat shock protein 70, isoform 2; BiP; annexin II; protein phosphatase 1 catalytic subunit, beta isoform; GDP dissociation inhibitor 2; and ras related nuclear protein (RAN). Top panel of each figure corresponds to MS1 reconstructed ion chromatograms for each peptide identified. The “no peptide” condition (CTRL) was set as a reference point. Red arrows correspond to the scan time at which the peptide sequence was identified by fragmentation. Bottom panels correspond to MS2 for different charge states of the identified peptide. Peaks

in black are unmatched peaks for each peptide sequence. Matched peaks are colored in red or blue.

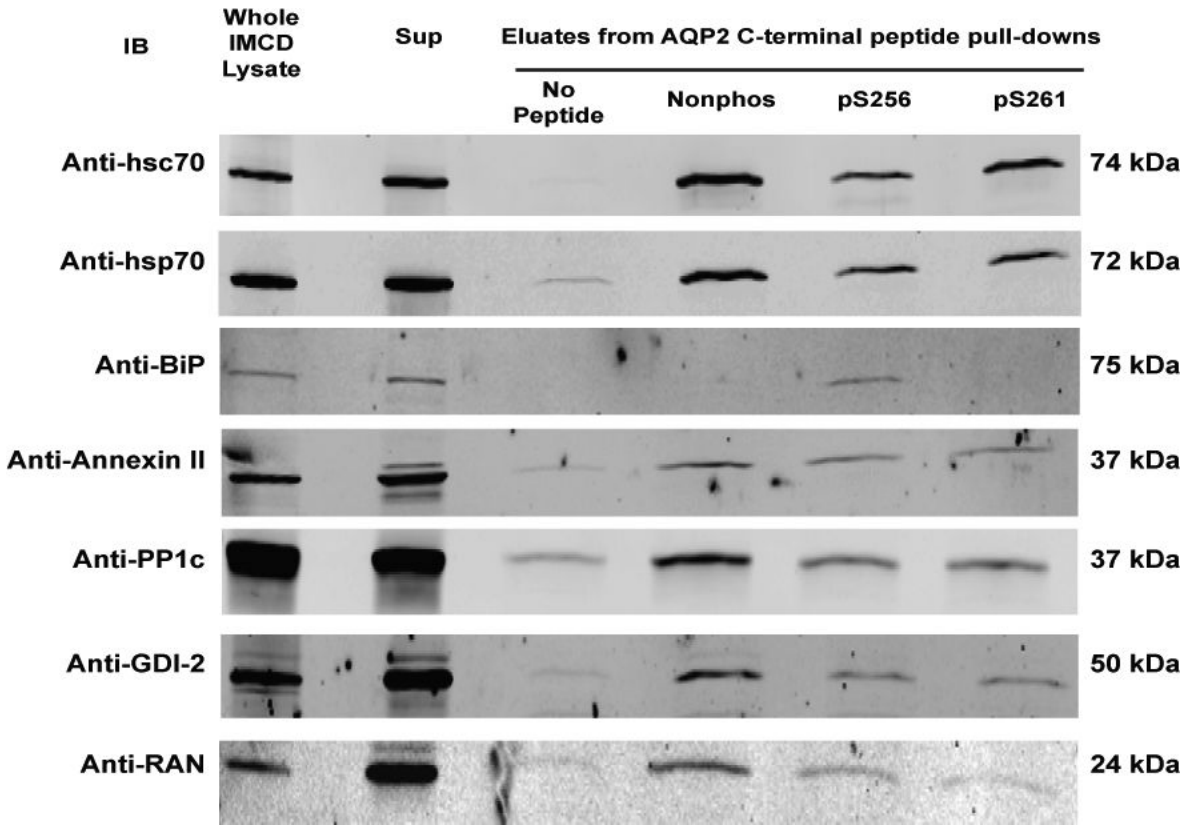

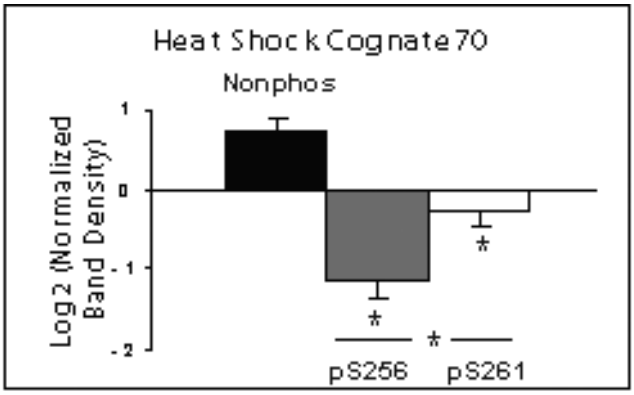

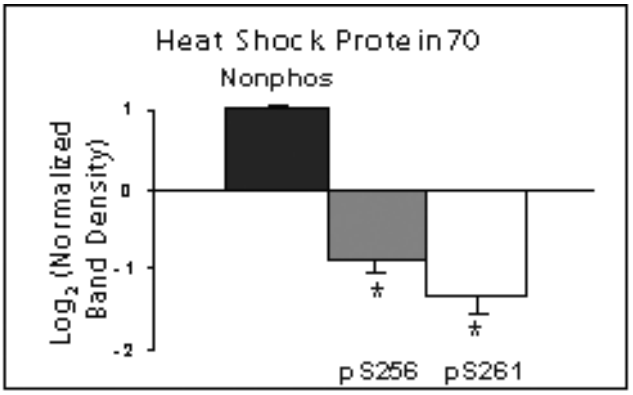

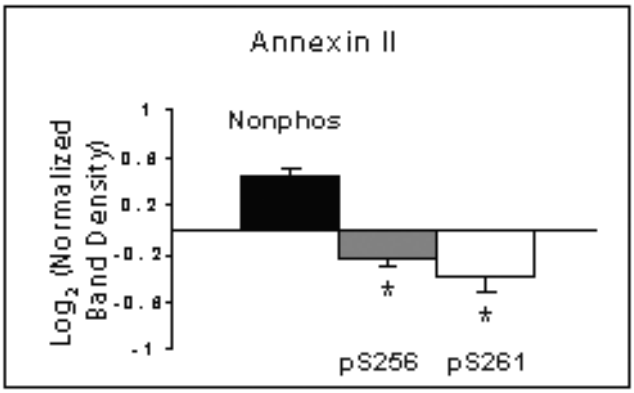

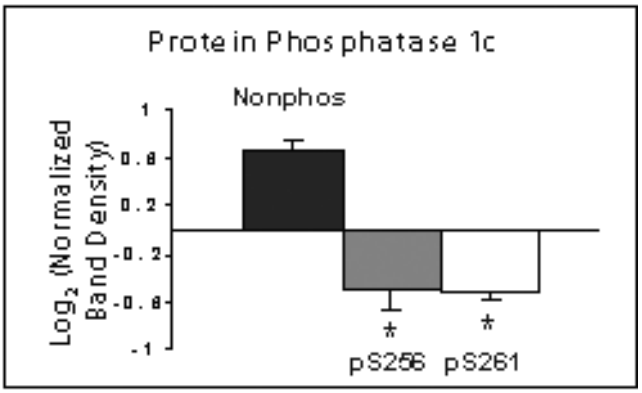

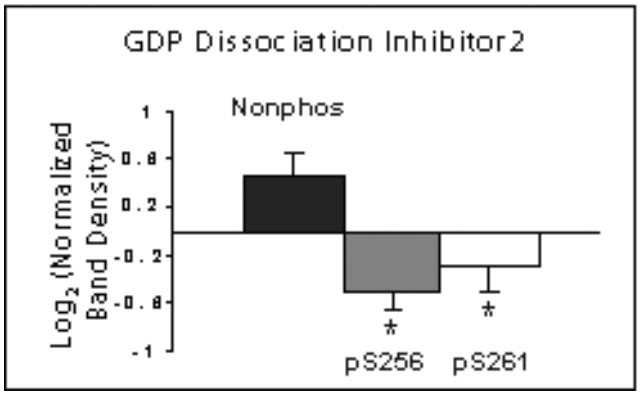

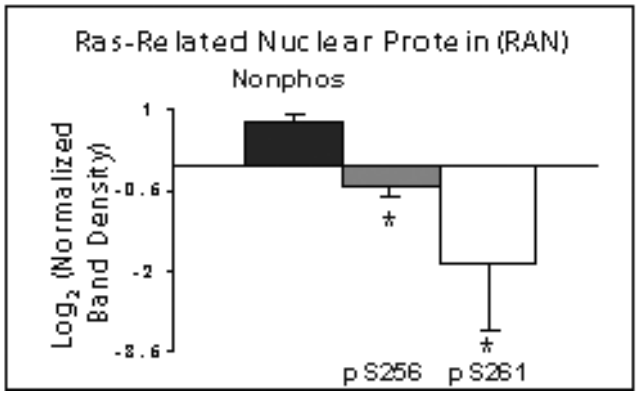

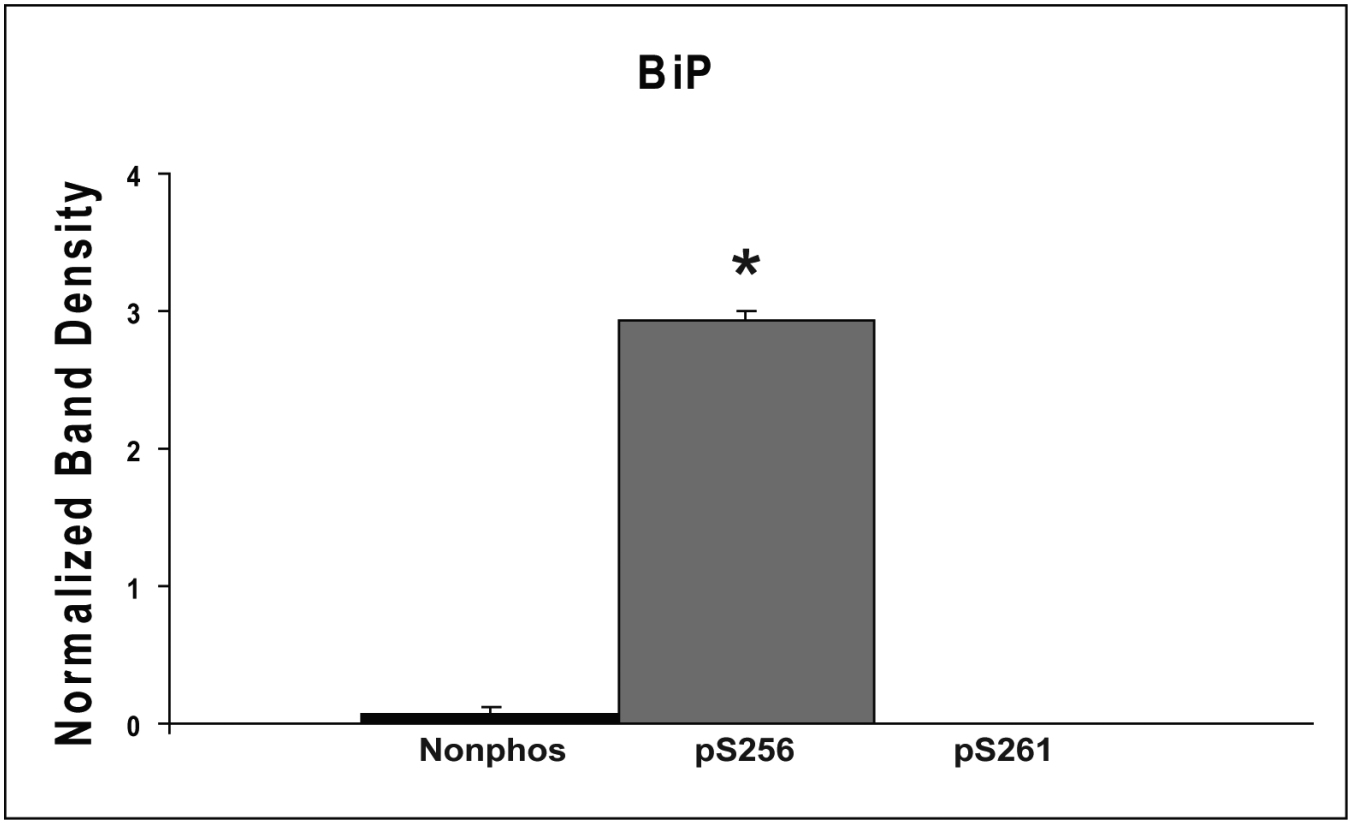

Figure 3. Confirmation of mass spectrometric results by immunoblotting

A) Whole cell IMCD homogenate (ranging 10−20 μg total protein) was used as a positive control. A second positive control consisted of cytosol isolated from native IMCD cells (the starting material for peptide pull-downs). Shown are representative blots: hsc70, n=5; hsp70, n=3; BiP, n=3; annexin II n=4; protein phosphatase 1 catalytic subunit (PP1c), n=4; GDP dissociation inhibitor 2 (GDI-2), n=5; ras-related nuclear protein (RAN), n=4. B) Log2 quantification of differences in signal intensity in the eluates corresponding to each AQP2 COOH-terminal peptide pull-down. Band density was normalized in each scan against the average signal from the nonphospho, pS256, and pS261. The log2 value was taken for each normalized value. SEM bars are shown on plots. Statistical significance was determined by using ANOVA with Bonferroni comparison across multiple columns. An asterisk (*) indicates $p<0.05$. C) Quantification of differences in BiP signal intensity in the eluates from AQP2 COOH-terminal peptide pull-downs. Log2 values were not taken since some normalized signal intensities corresponding to the nonphospho- and pS261 peptides were close to zero.

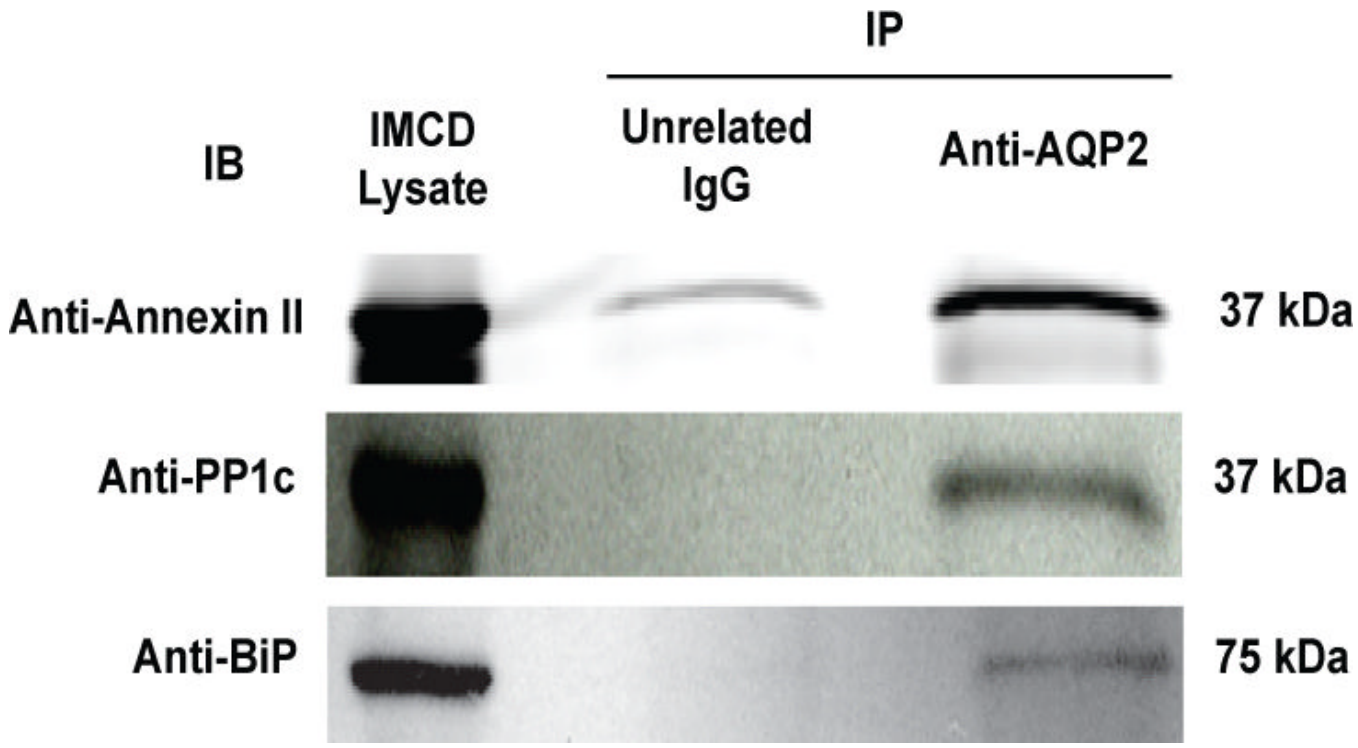

Figure 4. Immunoprecipitations from native IMCD

The eluates from AQP2 immunoprecipitations were probed by immunoblotting. Blots shown are representative of repeated experiments: annexin II, n=4; PP1c, n=4; BiP, n=2.

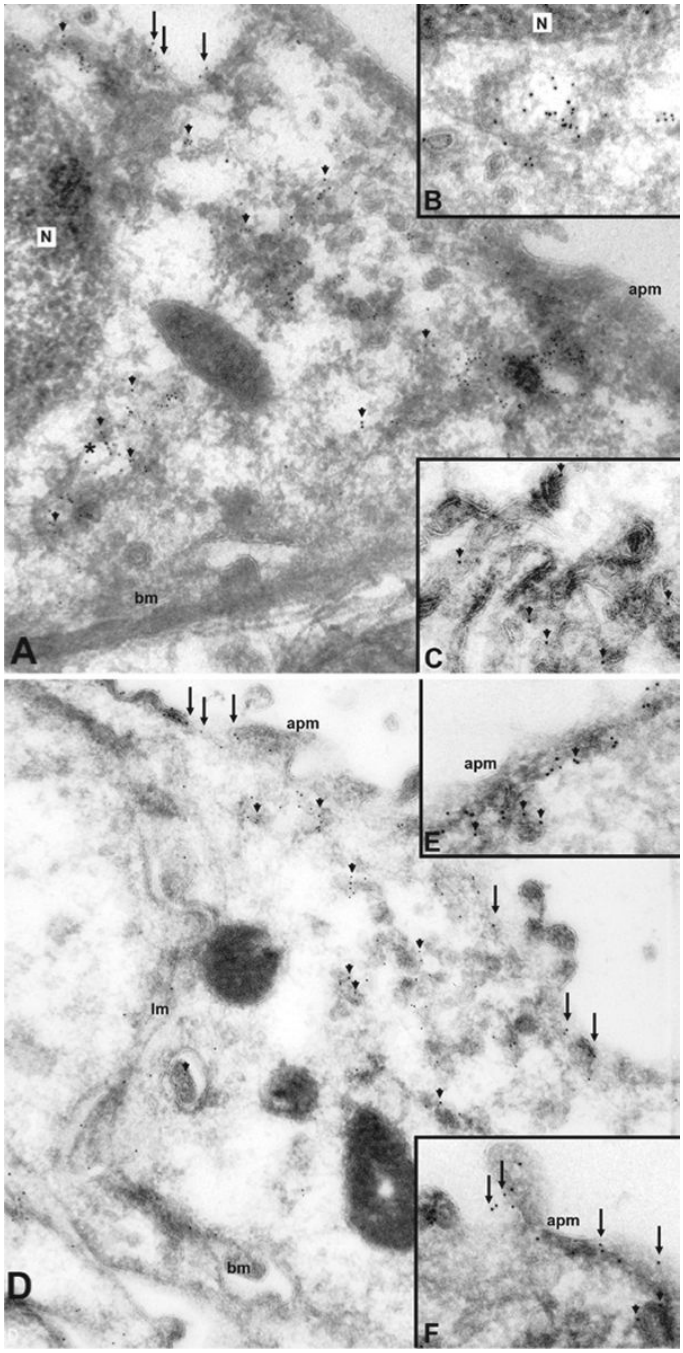

Figure 5. Immunogold electron microscopy of BiP in normal rat kidney

A) In inner medulla, BiP localizes both intracellularly (arrowheads) and to the apical plasma membrane (arrows) of collecting duct principal cells. Clusters of gold particles are observed in intracellular compartments structurally resembling the endoplasmic reticulum (*). At higher magnification (B) BiP labeling of the ER is more distinct, but there is also strong labeling associated with the Golgi network and vesicles (C). In the base of the inner medulla (D), BiP labeling is more prominent in the apical plasma membrane (arrows) but BiP is also clearly apparent in intracellular vesicles (arrowheads). At higher magnification, BiP labeling is observed both sub-apically (E, arrowheads) and in direct association with the apical plasma

membrane (F, arrows). N, nucleus; apm, apical plasma membrane; bm, basal membrane; lm, lateral membrane.

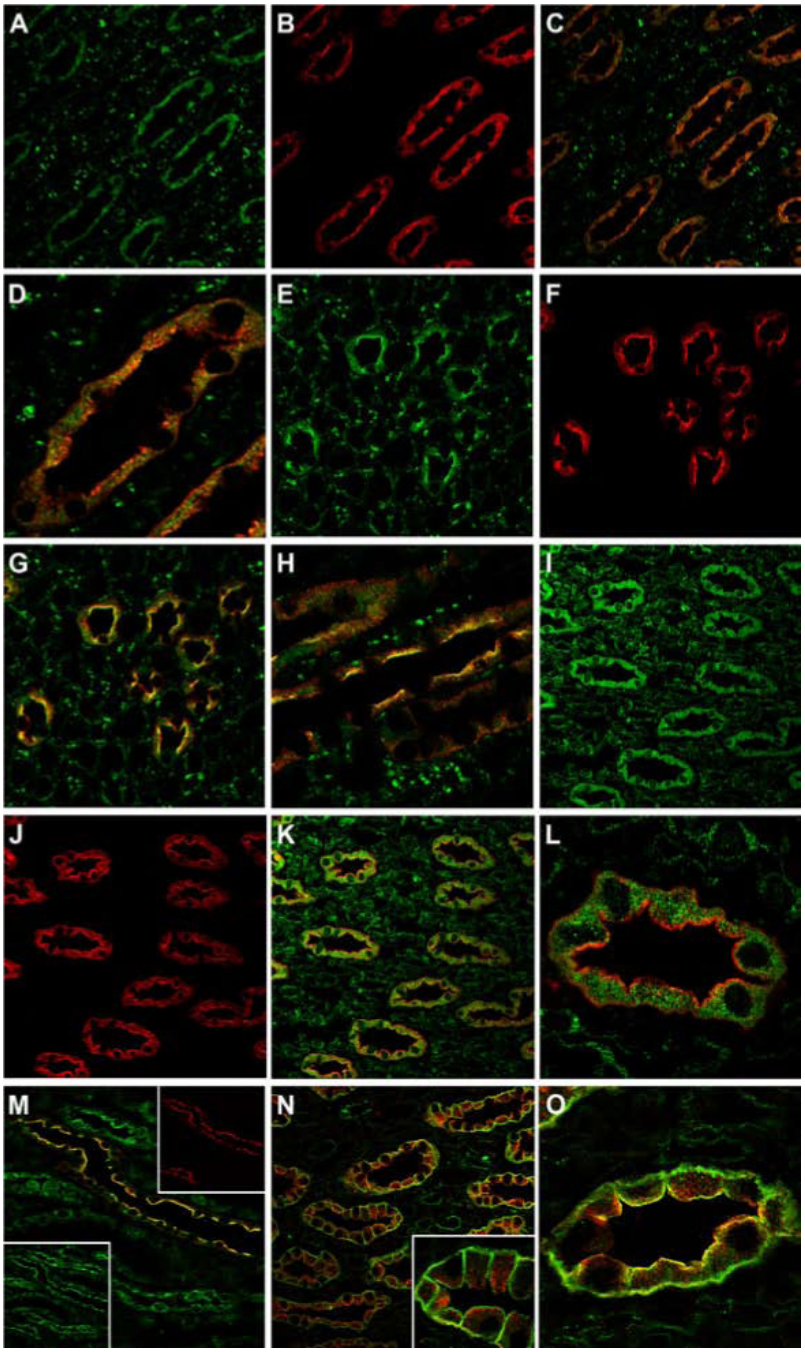

Figure 6. Confocal laser scanning microscopy of BiP, PP1c, and annexin II in normal rat kidney

In inner medulla, BiP (A, green) and AQP2 (B, red) are colocalized to collecting duct principal cells (C). At higher magnification (D) there is partial colocalization (yellow) of BiP and AQP2 within the cytoplasm. In the base of the inner medulla, both BiP (E, green) and AQP2 (F, red) colocalize (G) at the collecting duct apical plasma membrane. At higher magnification (H) this is much more apparent. In comparison, PP1c (I, green) and AQP2 (J, red) also colocalize to collecting duct principal cells (K). In the majority of IMCDs, PP1c (green) is localized intracellularly (L). In the cortical collecting ducts (M), AQP2 (red, inset) and PP1c (green, inset) colocalize predominantly at the apical plasma membrane. In the inner medulla (N), annexin II (green) is localized to collecting ducts along with AQP2 (red). At higher

magnifcation (inset) annexin II is localized predominanty in the apical and basolateral membrane domains. In the initial IMCD (O), annexin II (green) and AQP2 (red), partially colocalize (yellow) at the apical plasma membrane.

Table 1

Spectral counting of peptides corresponding to full-length proteins identified in eluates of AQP2 peptide pull-downs.

Protein	RefSeq ID	No peptide	Nonphos	pS256	pS261	Exp Number
Heat Shock Cognate 70 (hsc70)	NP_077327.1	1	16	8	×	1
		0	175	40	×	2
		0	551	145	417	3
		0	122	53	77	4
Heat Shock Protein 70 Isoform 1 (hsp70−1)	NP_997669.1	0	2	0	×	1
		0	1	1	×	2
		0	74	12	19	3
		2	31	30	20	4
Heat Shock Protein 70 Isoform 2 (hsp70−2)	NP_068635.1	2	5	2	×	1
		0	31	6	×	2
		0	145	24	88	3
		0	36	22	35	4
BiP	NP_037215.1	0	0	4	×	1
		0	18	68	×	2
		0	6	34	0	3
		0	2	24	0	4
Annexin II	NP_063970.1	1	4	1	×	1
		4	27	16	×	2
		14	34	28	34	3
		0	2	1	0	4
Protein Phosphatase 1 Catalytic Subunit (PP1c)	NP_037197.1	0	0	0	×	1
		0	7	4	×	2
		0	4	2	2	3
		0	1	0	0	4
GDP Dissociation Inhibitor 2 (GDI-2)	NP_058972.2	0	0	0	×	1
		0	4	0	×	2
		0	2	0	0	3
		0	1	1	0	4
Ras-Related Nuclear Protein (RAN)	NP_445891.1	0	0	0	×	1

Protein	RefSeq ID	No peptide	Nonphos	pS256	pS261	Exp Number
		0	0	0	×	2
		1	4	4	4	3
		0	2	1	1	4

Table 2

MS-based quantification of proteins that bound to AQP2 COOH-terminal peptides.

Protein name	Nonphos	pS256	pS261
hsc70	5.70 ± 0.27	3.70 ± 0.32***	3.87 ± 0.35***
hsp70 isoform 1	3.41 ± 0.44	2.4 ± 0.49	1.59 ± 0.43*
hsp70 isoform 2	4.17 ± 0.38	1.98 ± 0.60**	1.63 ± 0.58**
BiP	2.13 ± 0.57	5.36 ± 0.37***	0.23 ± 0.54*
annexin II	3.19 ± 0.32	2.11 ± 0.34*	2.09 ± 0.16*
PP1c	2.85 ± 0.98	1.61 ± 1.04	0.74 ± 0.57
GDI2	3.93 ± 1.25	1.06 ± 0.96	1.3 ± 1.34
RAN	1.9 ± 0.57	1.49 ± 0.25	0.72 ± 1.48

* $p < 0.05$

** $p < 0.01$

*** $p < 0.001$